

Memory Efficient LDDMM for Lung CT

Thomas Polzin^a, Marc Niethammer^b, Mattias P. Heinrich^c, Heinz Handels^c, and Jan Modersitzki^{a,d}

^aInstitute of Mathematics and Image Computing, University of Lübeck, Germany. ^bDepartment of Computer Science and Biomedical Research Imaging Center, University of North Carolina at Chapel Hill, USA. ^cInstitute of Medical Informatics, University of Lübeck, Germany. ^dFraunhofer MEVIS, Lübeck, Germany.
Contact: polzin@mic.uni-luebeck.de

Motivation

Why do we need lung registration?

Two main lung pathologies are:

- Lung cancer**, world-wide data [5]:
 - 1.825M incidences and 1.59M deaths per year (mortality rate of 87%)
 - Reason for 19.4% of all cancer-related deaths
- Chronic obstructive pulmonary disease (COPD)**, US-wide data [13]:
 - 24M individuals affected by COPD
 - COPD is fourth leading cause of death

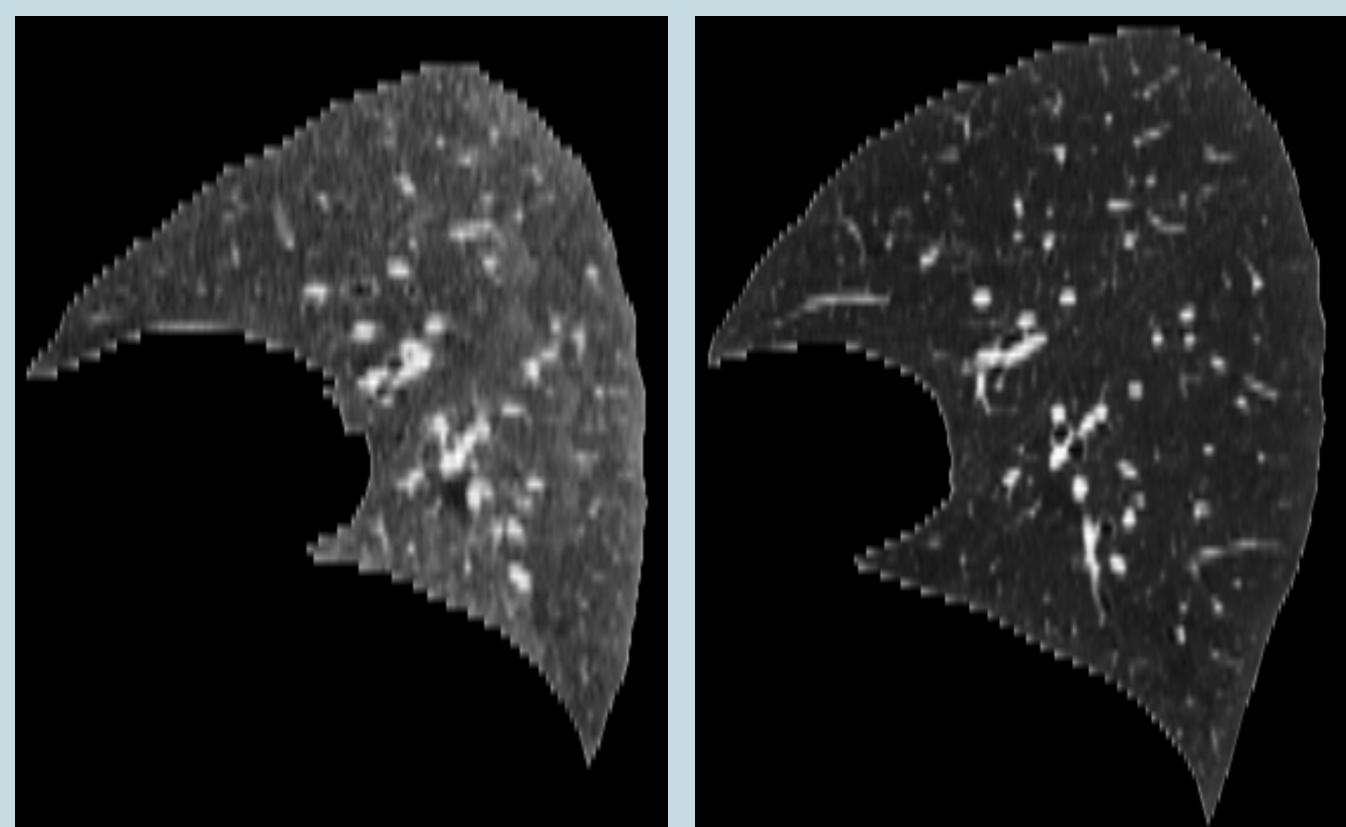
Possible applications of lung registration in diagnosis and therapy:

- Improved accuracy of radiotherapy [12]
- Alignment of follow-up data [12]
- Classification of COPD phenotypes [6]

Challenges

Why is lung registration difficult?

- **Large motion** during respiration (doubling in volume is possible) [4]
- Salient structures like vessels and bronchi are **small and repetitive**
- **Changing Hounsfield** units due to different densities, cf. figure below
- **Low-dose** acquisition results in **deteriorated image quality** [13]
- Movement within the lungs is smooth [12], i.e. diffeomorphic motion model is reasonable, but sliding motion occurs at, e.g., interface of lungs and ribcage [14]



Expiration

Inspiration



Movie with sagittal views of 4DCT data, image courtesy: Richard Castillo

LDDMM Background

Original Large Deformation Diffeomorphic Metric Mappings (LDDMM) model [1]: Given moving image I_0 and fixed image I_1 , find an optimal velocity field \hat{v} , that determines a diffeomorphic transformation ϕ , which aligns I_0 and I_1 ; $\hat{v}: \mathbb{R}^d \times [0, 1] \rightarrow \mathbb{R}^d$ is the minimizer of the following problem:

$$\hat{v} = \arg \min_{v: \phi_t = v_t(\phi_t)} \left(\int_0^1 \|v_t\|_V^2 dt + \frac{1}{\sigma^2} \|I_0 \circ \phi_1^{-1} - I_1\|_{L^2}^2 \right) \quad (1)$$

$$v_t(\cdot) := v(\cdot, t), \|v_t\|_V := \|Lv_t\|_{L^2}, Lv_t := (\gamma - \alpha\Delta)v_t; \alpha, \gamma, \sigma > 0$$

- Suitable model for registration of masked lung CTs
- Augmentation for sliding motion possible [14]

LDDMM as **optimal control** problem using advection equation for evolution of images [7]:

$$\hat{v} = \arg \min_v \left(\int_0^1 \|v_t\|_V^2 dt + \frac{1}{\sigma^2} \|I(1) - I_1\|_{L^2}^2 \right) \quad (2)$$

$$\text{s.t. } \partial_t I + (\nabla_x I)^T v = 0, I(0) = I_0, I: \mathbb{R}^d \times [0, 1] \rightarrow \mathbb{R}$$

- LDDMM is already successfully used for lung CT registration, but is **computationally demanding** [16]
- Memory requirements and runtime might prohibit use on standard PCs, e.g. in [16] run times of up to three hours are reported for moderately sized data of $256 \times 192 \times 180$ voxels using 32 CPUs and 128 GB RAM

Contributions

- We exploit the inherent smoothness of v by choosing a coarser discretization than given by image resolution
- Therefore, memory consumption and runtime are substantially reduced
- Registration accuracy is conserved by proper interpolation and computation of the **distance measure and its derivative** on full resolution [9]
- In particular, we use the well-suited **Normalized Gradient Fields** [11]:

Proposed LDDMM scheme

- Integrate the Normalized Gradient Fields (NGF) distance measure [11, 15]:

$$D(\varphi; I_0, I_1) := \int_{\Omega} 1 - \frac{\langle \nabla I_0(\varphi(\mathbf{x})), \nabla I_1(\mathbf{x}) \rangle_{\eta}}{\|\nabla I_0(\varphi(\mathbf{x}))\|_{\eta} \|\nabla I_1(\mathbf{x})\|_{\eta}} d\mathbf{x}, \quad (3)$$

$$\langle \mathbf{u}, \mathbf{v} \rangle_{\eta} := \eta^2 + \sum_{i=1}^d u_i v_i, \|\mathbf{u}\|_{\eta}^2 := \langle \mathbf{u}, \mathbf{u} \rangle_{\eta}, \eta > 0$$

- Adapting (2) to the transportation of maps yields the constraint

$$\partial_t \varphi + J_{\varphi} v = \mathbf{0}, \quad \varphi(\mathbf{x}, 0) = \mathbf{x}, \quad (4)$$

where J_{φ} denotes the spatial Jacobian of φ

- Full model ($\varphi_1 := \phi_1^{-1}$):

$$\hat{v} = \arg \min_v \left(\int_0^1 \|v_t\|_V^2 dt + \frac{1}{\sigma^2} D(\varphi_1; I_0, I_1) \right) \text{ s.t. (4)} \quad (5)$$

- Optimality conditions of Lagrange function [7] with $\lambda: \mathbb{R}^d \times [0, 1] \rightarrow \mathbb{R}^d$:

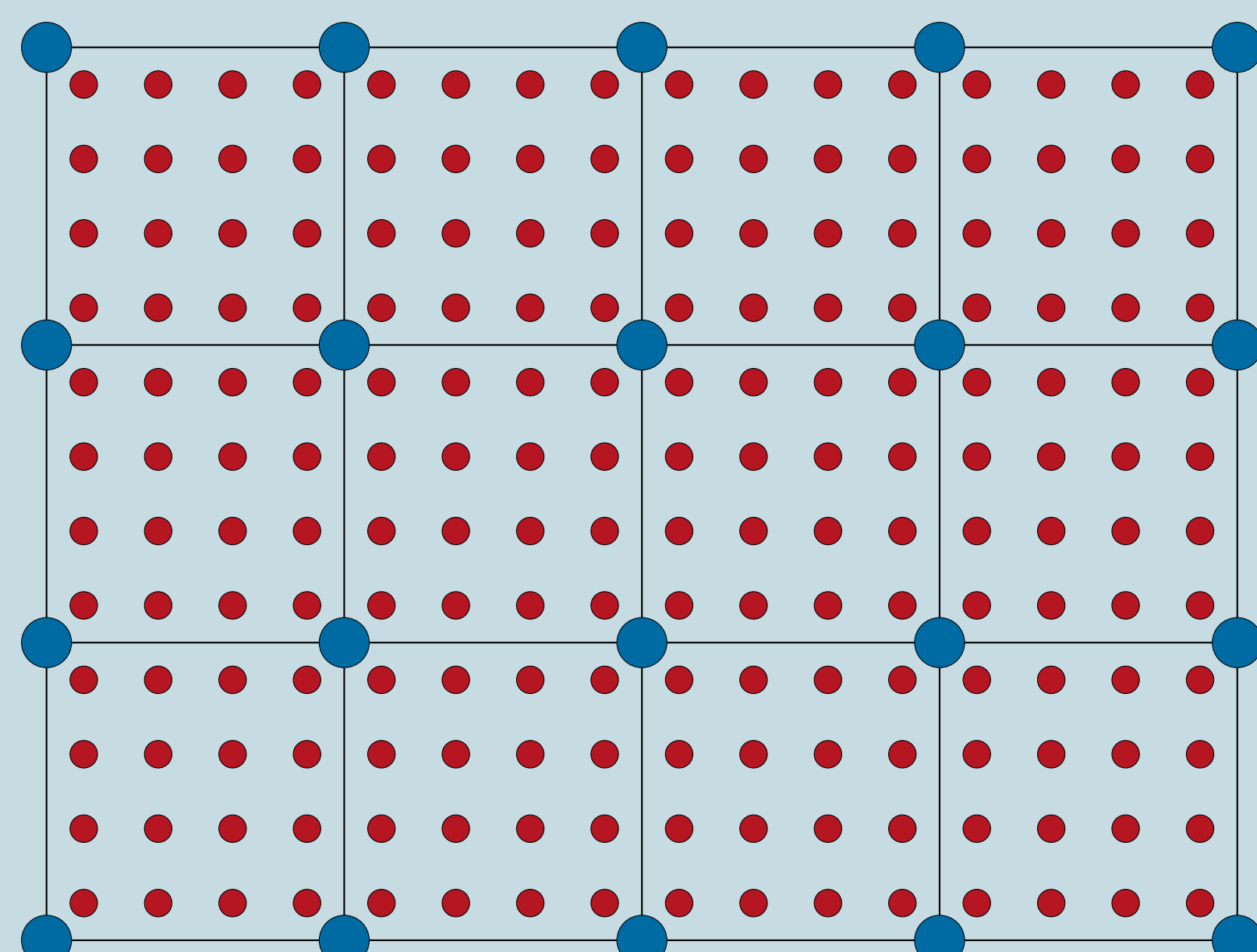
$$L^{\dagger} L v_t + J_{\varphi}^{\top} \lambda_t = \mathbf{0}, \quad (6)$$

$$\partial_t \varphi + J_{\varphi} v = \mathbf{0}, \quad \varphi(\mathbf{x}, 0) = \mathbf{x}, \quad (7)$$

$$\partial_t \lambda + J_{\lambda} v + \text{div}(v) \lambda = \mathbf{0}, \quad \lambda(\mathbf{x}, 1) = -\frac{1}{\sigma^2} \nabla_{\varphi} D(\varphi_1(\mathbf{x}); I_0, I_1) \quad (8)$$

Discretization and Numerical Optimization

- Use Discretize-Optimize approach, i.e. discretize objective and minimize it with numerical optimization [11]
- The discretized versions of (7) and (8) are solved with 4th order Runge-Kutta
- Problem (5) is solved numerically with a multi-level scheme on F levels
- Discrete images: $I_0, I_1 \in \mathbb{R}^{m_1 \times m_2 \times m_3}$
- Discretize v, φ on a nodal grid with $\bar{n} = n_1 n_2 n_3$ points and n_4 time steps: $\mathbf{v}, \varphi \in \mathbb{R}^{\bar{n} \times n_4}$, use $n_j \ll m_j, j = 1, 2, 3$ to reduce memory consumption and speed up computations



Visualization of image (red, small dots) and velocity grid (blue, large dots)

- Use trilinear interpolation matrix $\mathbf{P} \in \mathbb{R}^{\bar{m} \times 3\bar{m}}$, $\bar{m} := m_1 m_2 m_3$, to prolongate from coarse grid to image grid and \mathbf{P}^{\top} for reverse conversion
- \mathbf{P} is not stored [9] and only used for notational convenience
- Apply smoothing kernel $(\mathbf{L}^{\top} \mathbf{L})^{-1}$ to (6):

$$\mathbf{p} = \mathbf{v} + (\mathbf{L}^{\top} \mathbf{L})^{-1} (J_{\varphi}^{\top} \lambda) \quad (9)$$

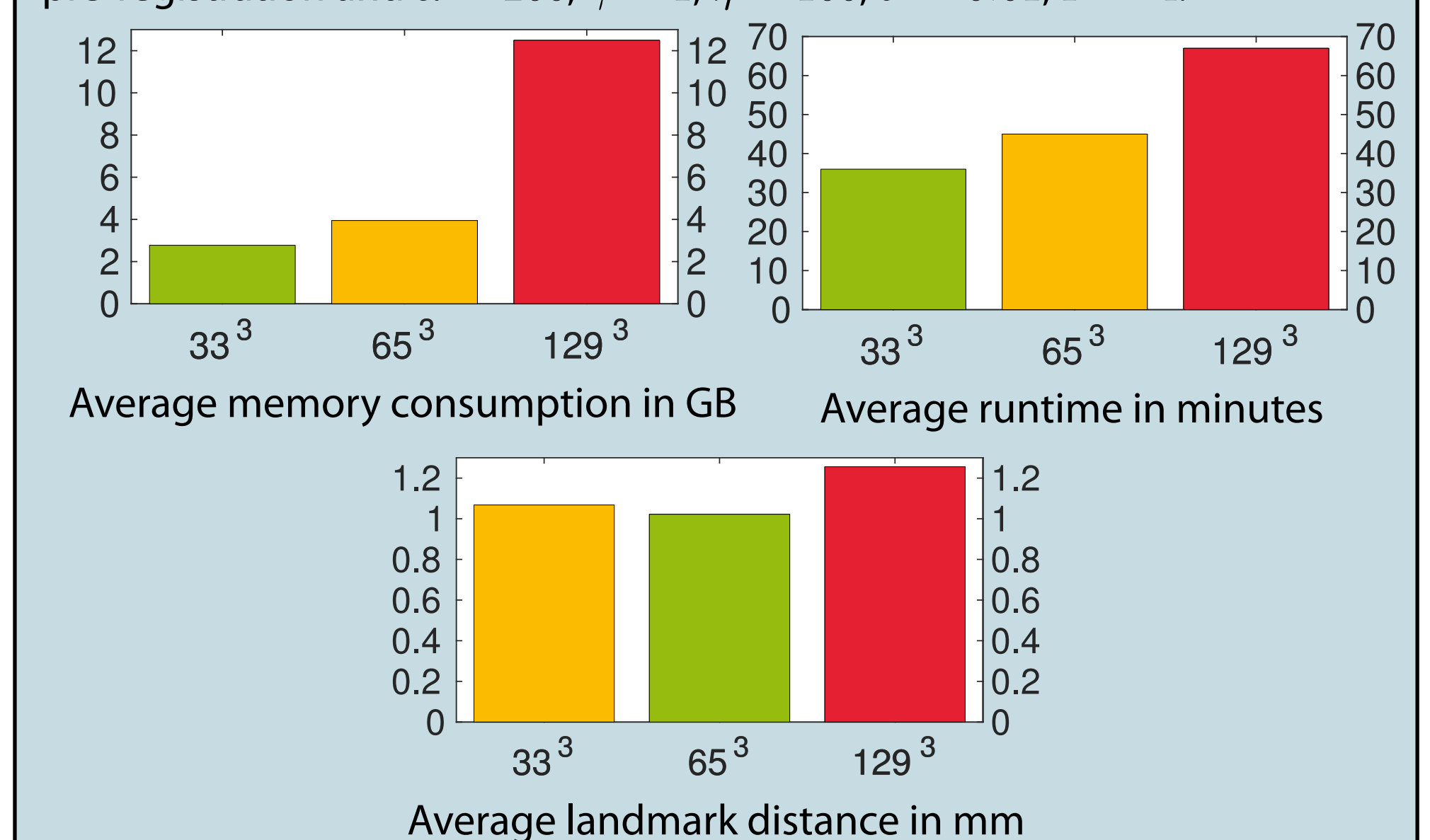
- Employ (9) as gradient for numerical optimization with limited memory BFGS and Armijo line search; use CG to solve the linear equation system

Material: DIR-Lab Lung CT data

- Registration of the publicly available DIR-Lab 4DCT [2] and COPD datasets [4], lung segmentations obtained with method [10]
- 20 inhale/exhale scan pairs and 300 landmarks per scan, that were annotated by medical experts
- Number of voxels in axial plane ranges from 256×256 to 512×512
- Slice thickness of 2.5 mm results in ca. 120 slices per case
- Distances of landmarks after registration are used for accuracy evaluation

Experiment 1: Influence of Velocity Grid Size

Influence of the velocity grid resolution on registration accuracy, memory consumption and runtime was investigated. We compared $\bar{n} = 33^3, 65^3, 129^3$ and registered inhale and exhale scans of 4DCT datasets. Used affine pre-registration and $\alpha = 200, \gamma = 1, \eta = 100, \sigma = 0.01, F = 4$.



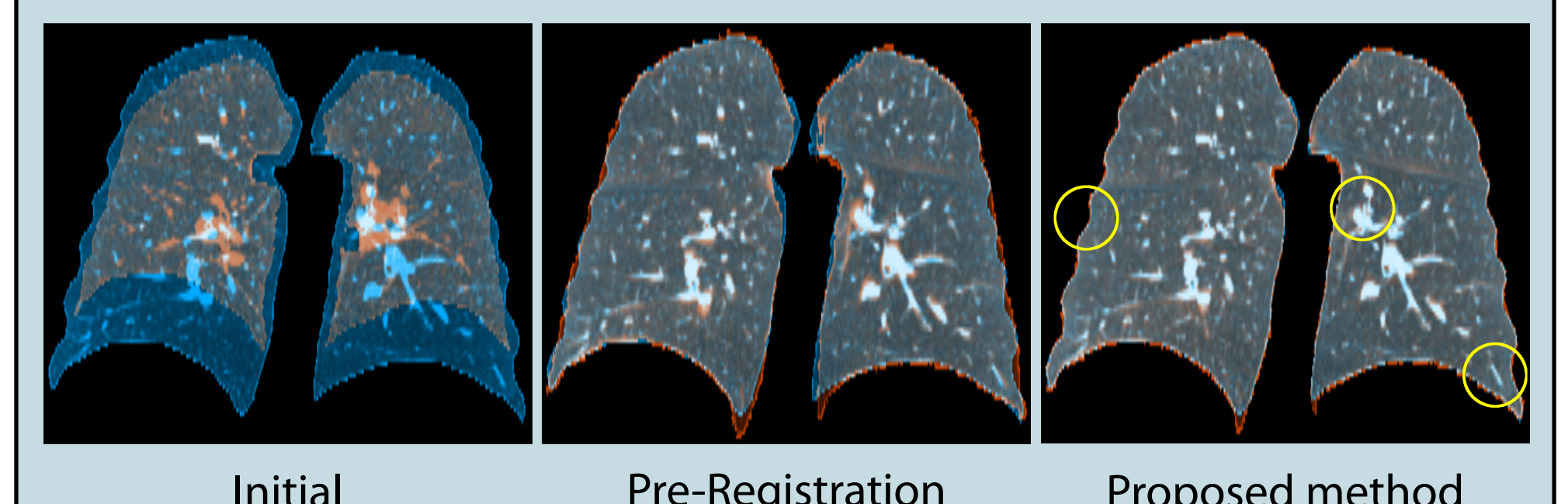
- Average landmark distances: 33^3 : 1.07 mm, 65^3 : 1.02 mm, 129^3 : 1.26 mm
- Accuracy of 33^3 and 129^3 grid points is significantly worse than for 65^3
- Memory requirements and runtime are moderate for 65^3

Experiment 2: Comparison to State-of-the-Art

We employed a keypoint-based [8] thin-plate spline pre-registration and removed keypoints that produced singularities in the deformation field. Parameters were fixed to $\alpha = 85, \gamma = 1, \eta = 100, \sigma = 0.1$ and $F = 5$. Motivated by the first experiment, we used $\bar{n} = 65^3$ on the finest level.

Case	Mean landmark distance in mm					proposed
	Initial	MILO [3]	MRF [8]	NLR [15]	Pre-Reg.	
COPD1	26.34	0.93	1.00	1.33	1.15	0.90
COPD2	21.79	1.77	1.62	2.34	2.18	1.55
COPD3	12.64	0.99	1.00	1.12	1.19	1.03
COPD4	29.58	1.14	1.08	1.54	1.32	0.94
COPD5	30.08	1.02	0.96	1.39	1.18	0.85
COPD6	28.46	0.99	1.01	2.08	1.27	0.94
COPD7	21.60	1.03	1.05	1.10	1.32	0.94
COPD8	26.46	1.31	1.08	1.57	1.47	1.12
COPD9	14.86	0.86	0.79	0.99	1.02	0.88
COPD10	21.81	1.23	1.18	1.42	1.51	1.17
Average	23.36	1.13	1.08	1.49	1.36	1.03
p-value	$4.8 \cdot 10^{-7}$	$5.5 \cdot 10^{-3}$	0.054	$9.5 \cdot 10^{-4}$	$1.5 \cdot 10^{-5}$	-

- The proposed method achieved the lowest average landmark errors published on the DIR-Lab COPD dataset
- Registrations took on average 46 minutes and used at most 5.9 GB of RAM
- A qualitative result is given in the following coronal overlays of fixed image (orange) and transformed moving image (blue)



Aligned structures appear gray or white due to addition of RGB values. Yellow circles highlight improvements.

Summary and Conclusion

- Presented **memory efficient LDDMM** scheme that exploits smoothness of velocity and transformation fields
- Discretization of the velocity and transformation fields with about one fourth of the image resolution reduces memory requirements substantially and speeds up computations whilst maintaining **diffeomorphic solutions and highly accurate image alignment**
- Integrated **NGF distance**, that is well-suited for lung CT registration
- Applied the method to 20 publicly available lung CT datasets and achieved results that outperform state-of-the-art methods

[1] Beg, M.F., et al.: Computing large deformation metric mappings via geodesic flows of diffeomorphisms. IJCV 61(2), 139–57 (2005)
 [2] Castillo, E., et al.: Four-dimensional deformable image registration using trajectory modeling. Physics in Medicine and Biology 55(11), 305–327 (2010)
 [3] Castillo, E., et al.: Computing global minimizers to a constrained B-spline image registration problem from optimal 11 perturbations to block match data. Med Phys 41(4), 041904 (2014)
 [4] Castillo, R., et al.: A reference dataset for deformable image registration spatial accuracy evaluation using the COPDgene study archive. Phys Med Biol 58(9), 2861–77 (2013)
 [5] Ferlay, J., et al.: Cancer incidence and mortality worldwide: Sources, methods and major patterns in GLOBOCAN 2012. International J. of Cancer 136(5), E359–E386 (2015)
 [6] Galbán, C.J., et al.: CT-based biomarker provides unique signature for diagnosis of COPD phenotypes and disease progression. Nature Medicine 18, 1711–1715 (2012)
 [7] Hart, G.L., et al.: An optimal control approach for deformable registration. In: IEEE CVPR Workshops. pp. 9–16 (2009)

[8] Heinrich, M.P., et al.: Estimating Large Lung Motion in COPD Patients by Symmetric Regularised Correspondence Fields. In: Navab, N., Hornegger, J., Wells, W.M., Frangi, A.F. (eds.) MICCAI 2015. pp. 338–345. Springer (2015)
 [9] König, L., Rühaak, J.: A fast and accurate parallel algorithm for non-linear image registration using Normalized Gradient fields. In: IEEE ISBI. pp. 580–583 (2014)
 [10] Lassen, B., et al.: Lung and Lung Lobe Segmentation Methods at Fraunhofer MEVIS. In: Proceedings of the Fourth International Workshop on Pulmonary Image Analysis. pp. 185–199 (2011)
 [11] Modersitzki, J.: FAIR: Flexible Algorithms for Image Registration. SIAM (2009)
 [12] Murphy, K., et al.: Evaluation of registration methods on thoracic CT: The EMPIRE10 challenge. IEEE Transactions on Medical Imaging 30(11), 1901–1920 (2011)
 [13] Regan, E.A., et al.: Genetic Epidemiology of COPD (COPDgene) Study Design. COPD 7, 32–43 (2011)

[14] Risser, L., et al.: Piecewise-diffeomorphic image registration: Application to the motion estimation between 3D CT lung images with sliding conditions. Med Image Anal 17(2), 182–93 (2013)
 [15] Rühaak, J., Heldmann, S., Kipshagen, T., Fischer, B.: Highly accurate fast lung CT registration. In: SPIE 2013, Medical Imaging. pp. 86690Y–1–9 (2013)
 [16] Sakamoto, R., et al.: Detection of time-varying structures by Large Deformation Diffeomorphic Metric Mapping to aid reading of high-resolution CT images of the lung. PLoS ONE 9(1), 1–11 (2014)



Get the poster!